

Design, synthesis, and anti-bacterial activities of piperazine based phthalimide derivatives against superbug-Methicillin-Resistant *Staphylococcus aureus*

H. S. Nagendra Prasad^{a*}, A.P.Ananda^{b,c}, Amogh Mukarambi^a, Navyatha Prashanth Gaonkar^a, S. Sumathi^d, H. P. Spoorthy^e and P. Mallu^a

^aDepartment of Chemistry, Sri Jayachamarajendra College of Engineering, JSS Science and Technology University, Mysuru-570006, India

^bCentre for Research and Evaluation, Bharathiar University, Coimbatore-641046, India

^cGanesh Consultancy and Analytical Services, Mysuru-570016, India

^dDepartment of Biochemistry, Biotechnology and Bioinformatics, Avinashilingam institute for Homescience and higher education for Women, Coimbatore-641043, India

^eDepartment of Microbiology, JSS College of Arts, Commerce and Science (Autonomous), Ooty Road, Mysuru-570002, India

CHRONICLE

Article history:

Received March 21, 2022

Received in revised form

April 20, 2022

Accepted September 26, 2022

Available online

September 26, 2022

Keywords:

Phthalimide derivative

MRSA

Molecular docking

Cytotoxicity

ABSTRACT

A series of piperazine-based phthalimide derivatives 5 (a-l) were synthesized and extensively characterized using a variety of spectrum methods, including LC-MS, ¹H-NMR, ¹³C-NMR, and FT-IR. All the derivatives were examined for their physicochemical, pharmacokinetic, bio-activity score, and PASS analysis. The 5e piperazine-based phthalimide derivative demonstrated promising antibacterial activity against methicillin-resistant *Staphylococcus aureus* (MRSA) in the *in vitro* antibacterial studies. In comparison to streptomycin and bacitracin (10 µg/mL), the minimum inhibitory concentration of 5e against MRSA was discovered to be 45±0.15 micro g/ml. The anti-MRSA activity was validated with membrane damage studies by using SEM, and in silico docking studies were against 3VMT and 6FTB proteins of MRSA. In the toxicity study, 5e derivatives were evaluated against L6 cell lines. The results of the studies show the synthesized 2-(2-(4-(4-chlorophenyl) sulfonyl) piperazin-1-yl) ethyl) isoindoline-1,3-dione (5e) can be used for the development of anti-MRSA drugs.

© 2023 by the authors; licensee Growing Science, Canada.

1. Introduction

Staphylococcus aureus is an important opportunistic pathogen responsible for many human infections globally.¹ These infections are at sites of lowered host resistance causing the infection through damaged skin (surgical site infection) or mucous membrane (ventilator-associated pneumonia).² Several studies have been done to decipher the specific molecular determinants involved in the virulence of *S. aureus* and its interaction with the host. Antibiotics³⁻⁴ was discovered at a crucial juncture in human history, changing medical research for the treatment of parasitic, fungal, and bacterial infections. Infectious diseases are a major public health issue that affects large sections of the global population.⁵ However, the efficacy of these wonder drugs against their intended microorganisms is declining due to the rapid development of resistance. Most hospital-acquired infections are caused by ESKAPE pathogenic bacteria (*Enterococcus faecium*, *Staphylococcus aureus*, *Klebsiella pneumoniae*, *Acinetobacter baumannii*, *Pseudomonas aeruginosa*, and *Enterobacter* species).⁶ Many MRSA clones have developed resistance to drugs such as erythromycin⁷, clindamycin⁸, ciprofloxacin⁹, tetracycline¹⁰, and others. Except for a few outbreaks of multidrug-resistant CA-MRSA, most CA-MRSA strains have not developed resistance to additional drugs.¹¹ Although various medicines have been shown to be successful in the treatment of MRSA infection, concerns have been raised about the formation of widespread resistance in MRSA to various antibiotics, such as

* Corresponding author.

E-mail address nprasadjss@gmail.com (H. S. Nagendra Prasad)

vancomycin, linezolid, and daptomycin. It is critical to find and develop new antibiotics with unique modes of action to combat MRSA.¹²⁻¹⁴

Piperazine is an organic heterocyclic compound with a six-membered ring containing two nitrogen heteroatoms at the C1 and C4 positions.¹⁵ Due of the various applications of heterocyclic compounds in agriculture and other areas, they play a significant role in nature.¹⁶ According to scientific literature the combinations of piperazine with various heterocyclic moieties.¹⁷ The piperazine compound is the backbone of many biologically potent molecules. piperazine derivatives belong to a very wide range of compounds with good pharmacore properties. Initially, piperazine was used as the anthelmintic, presently; commercially available drugs contain piperazine moieties as an important part of drug structure.¹⁸ Phthalamide is a phthalic acid imido derivative. Imide is a functional group in organic chemistry that consists of two carbonyl groups linked to nitrogen.¹⁹ These chemicals are structurally related to acid anhydrides and they are hydrophobic and neutral, allowing them to cross biological membranes in vivo. Phthalamide derivatives were shown to have antibacterial properties in several studies.²⁰ Anthelmintic action can be found in phthalamide derivatives of amino acid analogues. The utility of phthalamides and their derivatives is becoming increasingly popular.²¹ They have been discovered to be useful as inhibitors of tumour necrosis factor production. Many types of alkaloids and pharmacophores have been synthesised using phthalamides as starting materials or intermediates.²² To overcome the problem with Methicillin resistant *S. aureus*, the semisynthetic antibiotic was developed, which is derived from piperazine and phthalamide combinations.

2. Results and Discussions

2.1. Pharmacophore model, ADME, and BBB analysis of synthesized compounds

There are three parts to the designed molecules. Part A is a phthalamide with just oxygen as an electron donor and a sulfonyl of piperazine moiety (as a hydrogen acceptor/donor unit [HAD]) with promising bioactivity to perform the physicochemical, pharmacokinetic, and pharmacodynamic parameters represented in **Fig. 1**. We generated a variety of substitutions at thioamide piperazine with different types of phenyl groups to study the depth of the physicochemical behaviour of the synthesized compounds.

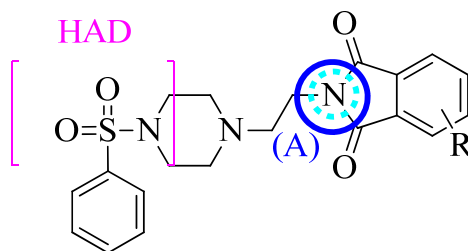


Fig.1. Pharmacophore model of synthesized compounds 5(a-l).

Table. 1. *In silico* scores of physicochemical and pharmacokinetic parameters of the synthesized 5(a-l).

Comp	miLog<5	TPSA (oA)	MW<500	n-ON<10	n-OHNH<5	n-rotb	MV	%ABS	Vio<1	BBB
5(a)	3.17	45.55	395.53	5	0	5	359.82	93.29	0	0.136
5(b)	2.80	79.69	413.50	7	0	5	358.89	81.50	0	0.129
5(c)	-0.92	102.75	414.46	8	0	5	347.61	73.56	0	0.135
5(d)	1.88	99.92	415.47	8	1	5	350.35	74.53	0	0.120
5(e)	3.03	79.69	433.92	7	0	5	355.87	81.51	0	0.093
5(f)	3.01	79.69	433.92	7	0	5	355.87	81.51	0	0.093
5(g)	2.98	79.69	433.92	7	0	5	355.87	81.51	0	0.093
5(h)	3.64	79.69	468.36	7	0	5	369.40	81.51	0	0.085
5(i)	2.52	79.69	417.46	7	0	5	347.26	81.51	0	0.101
5(j)	3.16	79.69	478.37	7	0	5	360.21	81.51	0	0.097
5(k)	3.44	79.69	525.37	7	0	5	366.32	81.51	1	0.089
5(l)	1.91	125.52	458.50	10	0	7	382.46	65.71	0	0.135

The portal (DOI: <http://www.molinspiration.com>)²³ was used to investigate the physico-chemical properties of the prepared compounds. The **Table 1** shows physico-chemical parameters such as clogP, clogS, drug-likeness, total surface area, polar surface area, and H-acceptor and H-donor parameters. The compounds' acceptability was further analyzed using Lipinski's rule of five, which is important for rational drug design. According to the Lipinski's rule of five compounds must have a molecular weight of ≤ 500 Daltons, ≤ 5 hydrogen bond donors, ≤ 10 hydrogen bond acceptors, and a logP of ≤ 5 .²⁴ Compounds that fulfil the criteria and have not more than one violation been categorized as drug-like compounds with good bioavailability. Poor ingestion and penetration are likely to occur when any two of the above-mentioned criteria are

broken. The PSA (polar surface area) of all the blended mixes was well within the acceptable (less 140Å²) and useful range. The compounds that were synthesized met Lipinski's criterion, indicating that they possessed the drug-like property (Supplementary figure S1).

2.2 Biological activity spectrum PASS analysis

The PASS software is a free web tool that may be used to determine the biological activity spectrum of a synthetic analogue and is used here to determine the activity. **Table 2** and **Supplementary Table S1** contain the findings of the synthesized analogue 5e. The compound 5e exhibits potent values of Passpiperantimyopathies (0.247), antineoplastic (melanoma) (0.239), antiprotozoal (Coccidial) (0.222), and antineoplastic (lung cancer) chemical 5 has potent values (0.199). The Pa and Pi values of the synthesized compound are excellent, indicating that the synthesized potent analogue (5) can be used as the futuristic therapeutic agent.

Table 2. Predicted biological activities of compounds 5e, Pa (probability “to be active”), Pi (probability “to be inactive”).

Activity	Pa	Pi
Anthelmintic (Fasciola)	0.192	0.069
Antiprotozoal (Coccidial)	0.222	0.148
Antiprotozoal (Trichomonas)	0.196	0.129
Antiprotozoal (Amoeba)	0.229	0.168
Antimyopathies	0.247	0.219
Antineoplastic (non-small cell lung cancer)	0.159	0.142
Antiseborrheic	0.199	0.185
Antineoplastic (lung cancer)	0.130	0.122
Antiseborrheic	0.199	0.185
Antineoplastic (lung cancer)	0.199	0.122

2.3. Synthesis and characterization of piperazine sulfonyl derivatives

In the present studies, a series of derivatives of piperazine phthalimide of 2-(2-(Piperazin-1-yl) ethyl) isoindoline-1, 3-dione (3) were synthesized (**Fig. 6**). In these twelve synthesized compounds, 5(a-l) were characterized using various spectral analyses such as ¹H NMR, LCMS, FTIR and ¹³C NMR. Spectral analyses were used to determine the structures of produced compounds (**Supplementary Figs 2-13**).²⁶ The results of the elemental analysis showed that the empirically measured values and theoretically estimated values were within 0.4 percent of each other. 2-(piperazine-1-yl) ethamine(1equi) yielded 2-(piperazine-1-yl) isoindoline-1,3-dione (3) was obtained by the reaction between commercially available phthalic anhydride (1) and 2-(piperazine-1-yl) ethamine(1equi).²⁷ By using various spectrum approaches the synthesized substances were characterized. The FT-IR spectra of all synthesised compounds were obtained in the 4000-400 cm⁻¹ range. The absorption bands at 1250 cm⁻¹ is attributed to the stretching vibration of C-N, absorption bands at 1760 cm⁻¹ are due to the presence of C=O stretch, -CH₂ rocking is visible at 760 cm⁻¹, and absorption bands at 1550 cm⁻¹ are due to the aromatic C=C stretch. In the supplementary file, spectral images are tabulated (Supplementary figure S14). In the ¹H-NMR spectra of synthesised compound 5e, the doublet peak at 7.8 is due to the aromatic proton, while the doublet peaks between δ 2.6 and 3.2 are attributed to the piperazine (Pip-H). Similarly, the protons of the aromatic group generated a doublet signal at δ 6.53- 8.98 ppm. The observed mass spectra indicate the molecular ion peak value of compound 5e agrees well with the molecular formula of synthesised compounds. The molecular ion peak for compound 5e was observed at m/z 433.91, which fits the molecular formula C₂₀H₂₀ClN₃O₄S.

2.4 Antibacterial activity of piperazine Derivatives against MRSA

The Resazurin method was used to assess the MIC of the synthesized 5(a-l) analogs. MRSA resistance was tested using the parent structure piperazine and phthalimide²⁸. The 5e has a remarkable MIC value of 45±0.15 µg/mL, which was validated by streptomycin and bacitracin 10 g/mL, which are both broad-spectrum antibiotics (**Table 3**). Disc diffusion was also used to determine 5e antibacterial activity in a dose-dependent manner. Piperazine 5e analogues inhibited zone in radius (ZIO) 4.82±0.02, 4.92±0.01, 5.32±0.02, 6.22±0.03, 6.82±0.02, and 7.68±0.03mm (**Figs. 2A & 2B**)²⁹⁻³⁰. The results indicate that the synthetic piperazine sulphonyl derivative due to its structural and chemical moieties is having significant results, according to the findings. The synthesized compound 5d shows moderately less activity due to the presence of aromatic ring with hydroxyl group. The remaining compounds also exhibit less activity towards MRSA due to the functional group present in the different positions; it is validated using molecular docking studies.

Table 3. MIC of the synthesized piperazine derivatives 5(a-l) against MRSA.

Synthetic compounds	Minimum inhibitory concentration (MIC) in µg/mL	Synthetic compounds	Minimum inhibitory concentration (MIC) in µg/mL
5a	70±0.48	5h	50±0.75
5b	64±0.19	5i	62±0.40
5c	62±0.21	5j	65±0.27
5d	48±0.14	5k	50±0.55
5e	45±0.15	5l	51±0.36
5f	49±0.48	Streptomycin	10 µg
5g	49±0.35	Bacitracin	10 µg

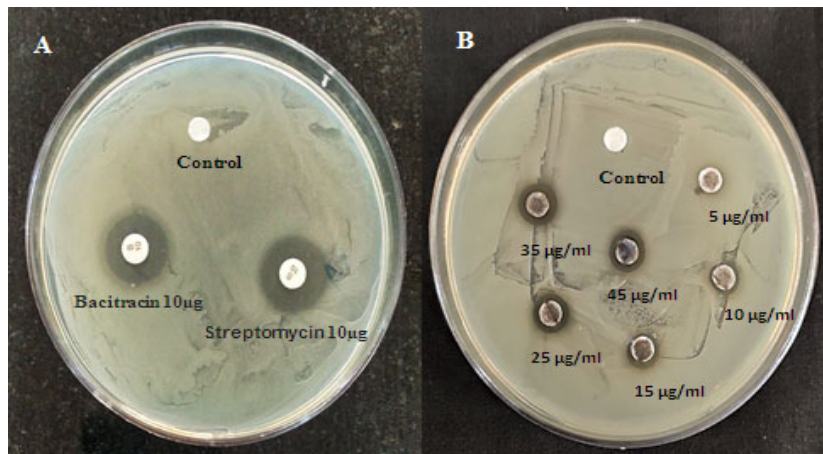


Fig. 2. Antimicrobial activity 5e against MRSA. (A) MRSA tested with standard drug bacitracin 10 µg/disc (10.36 ± 0.02) and streptomycin 10 µg/disc (11.84 ± 0.03) ZOI in mm, (B) 5e analogue.

2.5 Molecular docking for protein Glycosyltransferase with PDB ids 3VMT and 6FTB

The molecular docking predicted the active site conformations and binding energy of that compound with the electron-withdrawing group have strong inhibition potential³¹. In this study it was observed that the respective positions of the aromatic ring contain various substituents along with different orientations. The in-silico docking approach investigated the coupling mechanism and inclination of a small particle inside the receptor target protein's coupling site. The docked ligands were placed in ligand-receptor configurations based on their coupling affinity. In this work, 5e compound shows the various interactions (**Figs. 3A & 3B**) against two MRSA glycosyltransferase proteins, 3VMT and 6FTB. The strong interactions such as hydrogen, Vander Waals, and hydrophobic with potential amino acid residues promoted the binding of 5e during docking (**Table 4**). The compound 5e showed a good docking score against both the proteins when compared to the standard antibiotic streptomycin which contributed -10.656 kcal/mol and -7.879 kcal/mol, respectively, the ligand piperazine with phthalic anhydride, chloro groups (5e) contributed the highest docking score -6.941 kcal/mol with 3VMT protein and a significant score of -6.703 kcal/mol with 6FTB protein. The binding site of standard streptomycin compare with compound 5e is shown in **Figs. 3C & 3D**. The superior activity of these Cl analogs might be attributed to their high electronegativity and strong electron-withdrawing potential, and this is thoroughly observed in this series of compounds. ASP111, ARG117, ARG302, and GLY114, formed interaction with different protonated groups of compounds 5e against 3VMT protein and CCN136 and GLY131 establish the interaction with sulfonyl moiety in the compound against protein 6FTB, docking score along with glide energy of the synthesized molecules were tabulated in table 5 and binding site images of the all the molecule 5(a-l) provided in the supplementary data (**Supplementary figure S15**).

Table 4. Molecular docking scores of synthesized analogues, complex and antibiotic streptomycin against 3VMT and 6FTB protein

Protein	3VMT				6FTB			
	Docking Score	XP Gscore	Glide Energy (kcal/mol)	Glide Emodel (kcal/mol)	Docking Score	XP Gscore	Glide Energy (kcal/mol)	Glide Emodel (kcal/mol)
5a	-5.199	-5.203	-47.964	-55.517	-5.155	-5.158	-49.995	-56.332
5b	-6.271	-6.275	-49.335	-62.75	-5.912	-5.195	-42.995	-52.192
5c	-6.507	-6.51	-50.105	-62.74	-3.655	-3.553	-33.409	-43.297
5d	-6.227	-6.135	-53.893	-57.924	-5.865	-5.867	-41.356	-52.341
5e	-6.941	-6.143	-45.743	-59.634	-6.703	-6.706	-40.657	-49.39
5f	-5.593	-6.595	-50.775	-57.906	-6.258	-6.261	-45.579	-54.393
5g	-6.253	-6.256	-48.995	-63.38	-6.378	-6.38	-41.477	-45.812
5h	-5.002	-5.004	-53.78	-71.129	-6.14	-6.142	-41.215	-53.411
5i	-6.043	-6.746	-42.934	-53.305	-5.038	-5.041	-42.824	-52.249
5j	-5.254	-5.257	-49.691	-64.334	-5.751	-5.754	-41.149	-51.431
5k	-6.262	-4.266	-48.423	-62.502	-5.027	-5.029	-45.36	-61.916
5l	-5.107	-6.109	-51.159	-62.151	-5.34	-5.341	-44.63	-60.619
Streptomycin	10.656	10.828	59.987	77.87	7.879	7.517	55.213	69.461

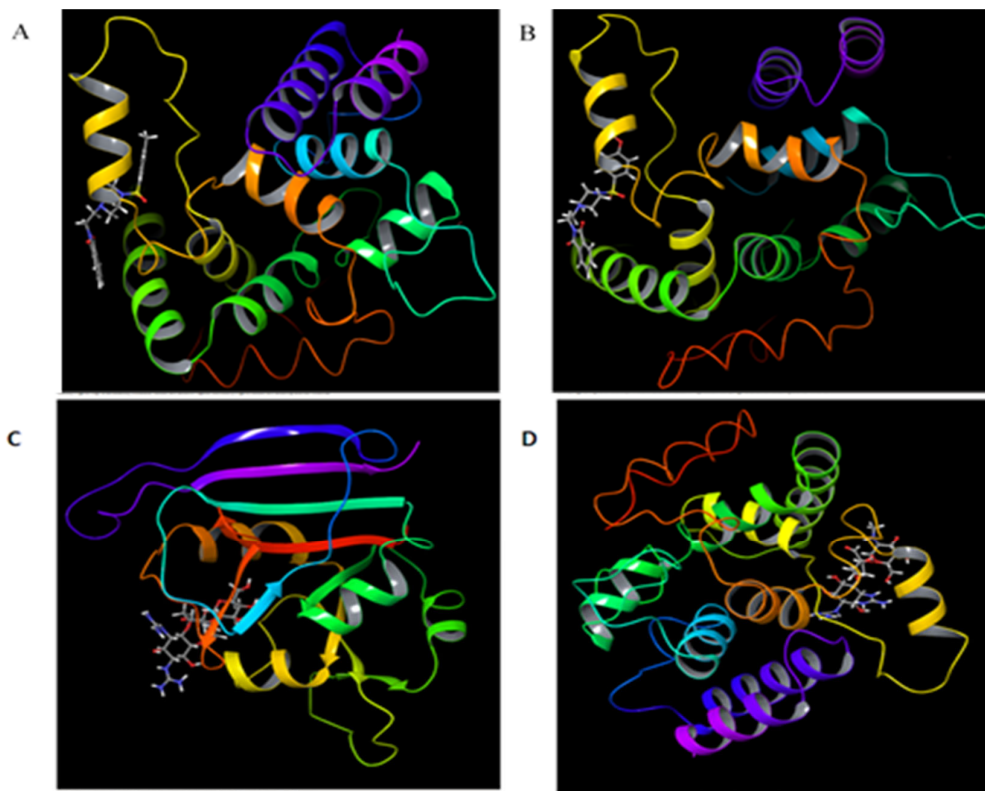


Fig. 3. Molecular docking proof for 3VMT (A), 6 FTB (B) and standard streptomycin (C, D) proteins of MRSA in the best pose at active sites of targets by 5e and streptomycin respectively (3D images).

2.6 Membrane damage

Due to its potent activity against superbug MRSA, piperazine sulfonyl derivative analogues were chosen to visualize cell membrane damage. In comparison with the control, the structural membrane of the 5e showed significant changes. The SEM indicated pores, breaks, and cracks in the treated MRSA compared to the untreated smooth control surface (**Fig 4**).⁴³ This indicates the bactericidal activity is due to the metal complex binding to the membrane or membrane-bound factors. Then it leads to cellular content leakage, which leads to cell death. This is an indication that the host is protected from the harmful inflammatory responses and give protection from the adverse inflammatory complications that can be induced during MRSA infection in the host.

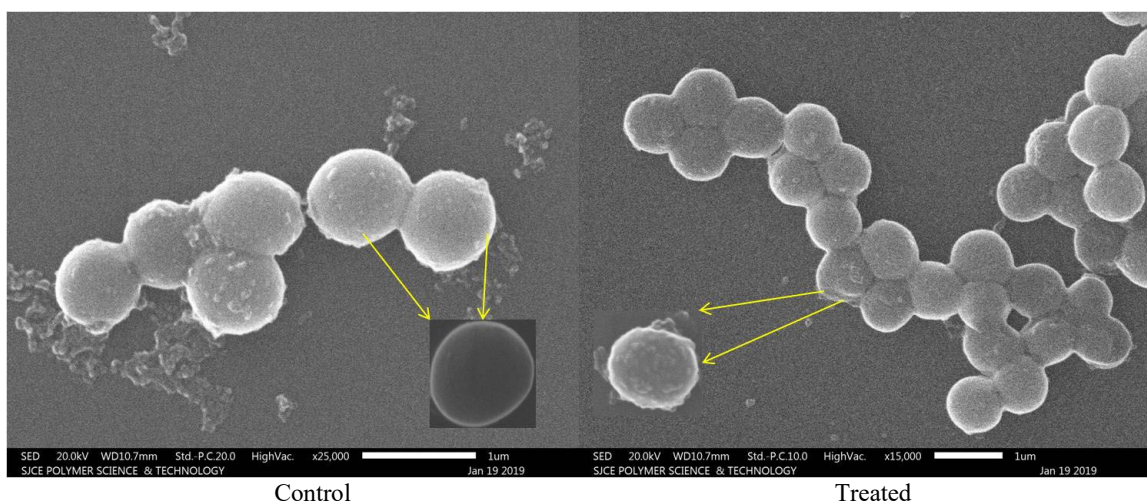


Fig. 4. Antibacterial activity of 5e was evidenced by cell membrane damage of MRSA. The MRSA was treated with a MIC value of 5e and without treated MRSA as control.

2.7. Toxic effect of piperazine sulfonyl derivative 5e

The anti-proliferative effect of 5e on skeletal muscle cells was investigated using MTT cytotoxicity test in the current investigation (L6 myotubes). The 5e chemical was chosen for the cytotoxicity assay since it was found to be a strong contender against MRSA. The data obtained indicated the synthesised 5e analogue had an IC₅₀ value of 225.50 µg/mL (Fig 5A & 5B)

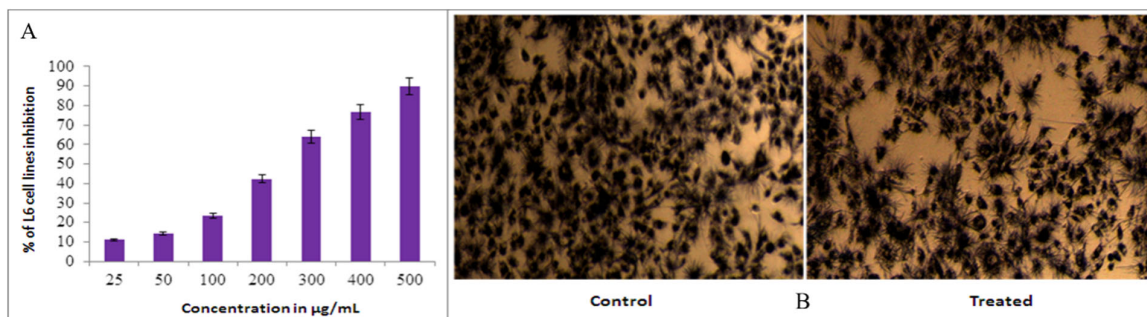


Fig.5. Toxicity of 5e. A. Represent the % inhibition L6 cell lines with respect to different concentrations of 5e. B. Images of control cell lines and treated cell lines.

3. Conclusion

In the present study, we design, synthesized twelve compounds 5 (a-l) and their structure was confirmed using various spectral technique such as NMR, LCMS and FTIR. 5e derivative of piperazine-based phthalimide shown remarkable antibacterial capability against MRSA. The anti-MRSA activity was measured by SEM analysis and validated with molecular docking proof against perilous pathogenic MRSA proteins 3VMT and 6FTB. The piperazine based phthalimide derivatives showed excellent anti-MRSA activity and could be considered a commendable candidate to study its potential as an effective therapeutic agent for the management of the MRSA infections.

Acknowledgements

The authors greatly thankful to Sri Jayachamarajendra College of Engineering (SJCE), JSS Science and Technology University, Mysuru and Ganesh Consultancy & Analytical Services, Mysuru for providing instrumentation facility.

Competing financial interests

The authors declare no competing financial interest.

4. Experimental

All chemicals were procured from Sigma Aldrich India. All the synthesis work was done with AR-grade solvents and reagents. For column chromatography, silica gel was obtained from Merk Pvt Limited Mumbai India. The IR spectrum was recorded using Agilent Cary 630 FT-IR spectrometer. All the spectra were run in the range 400–4000 cm⁻¹ at room temperature. The ¹H and ¹³C NMR spectrum was recorded in CDCl₃. All chemical shifts are reported in ppm relative to TMS. Mass spectroscopic analysis was performed in a Waters micro TOF QII mass spectrometer. The lyophilized reference *Staphylococcus aureus*-96 strain was obtained from Microbial Typing Culture Collection (MTCC), Chandigarh, India, and strains were cultured in recommended broth as per the revival procedure provided by MTCC. The required culture medium was purchased from Hi-Media Laboratories, Mumbai, India

4.1. Synthesis of piperazine ligands

4.1.1. Synthesis of 2-(2-(piperazine-1-yl) ethyl) isoindoline-1,3-dione (3)

In 25 mL methanol, isobenzofuran-1,3-dione (0.5g) (1) and 2-(piperazine-1-yl) ethamine (0.45g) (2) were refluxed for 6 hours, followed by adding 2-3 drops of glacial acetic acid to the reaction mixture. The completeness of the reaction was confirmed using TLC. In a rotary evaporator, the solvent was concentrated at 50°C before being rinsed with distilled water. The solid product was dried and recrystallized in methanol. The greenish-yellow product (3) was produced with good yields (Fig 6)

4.1.2. Synthesis of 2-(2-(4-(Phenylsulfonyl) piperazine-1-yl) ethyl) isoindoline-1,3-dione

In an ice bath, a solution of 2-(2-(piperazin-1-yl) ethyl) isoindoline-1, 3-dione (3) (0.5g) in DCM was cooled to 0-50°C. After adding three drops of triethylamine to the cool reaction mixture and stirring for ten minutes, several sulfonyl derivatives [4(a-l)] (Table 5) (0.2g) were added. For 6 hours, the reaction mixture was refluxed (figure 6). TLC was used to track the reaction's progress. The solvent was withdrawn under reduced pressure at the end of the reaction and re-extracted with ethyl acetate. The organic layer was then washed with Millipore water and 1 percent HCl. By passing the chemical via anhydrous sodium sulphate, it was de-moisturized.

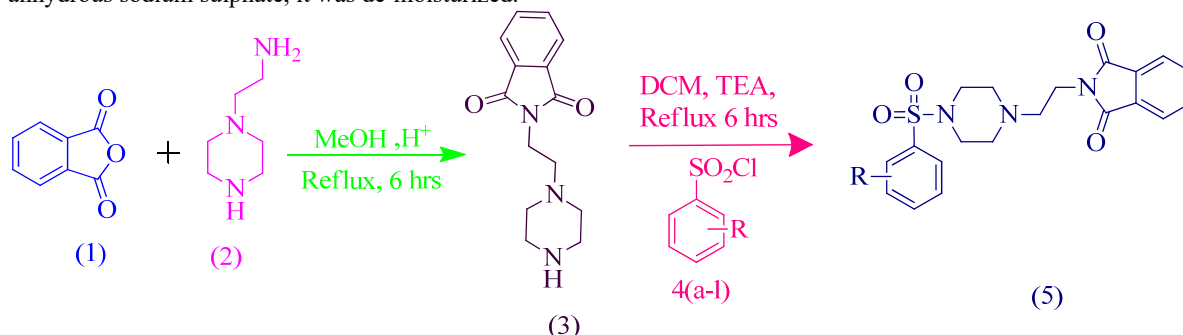
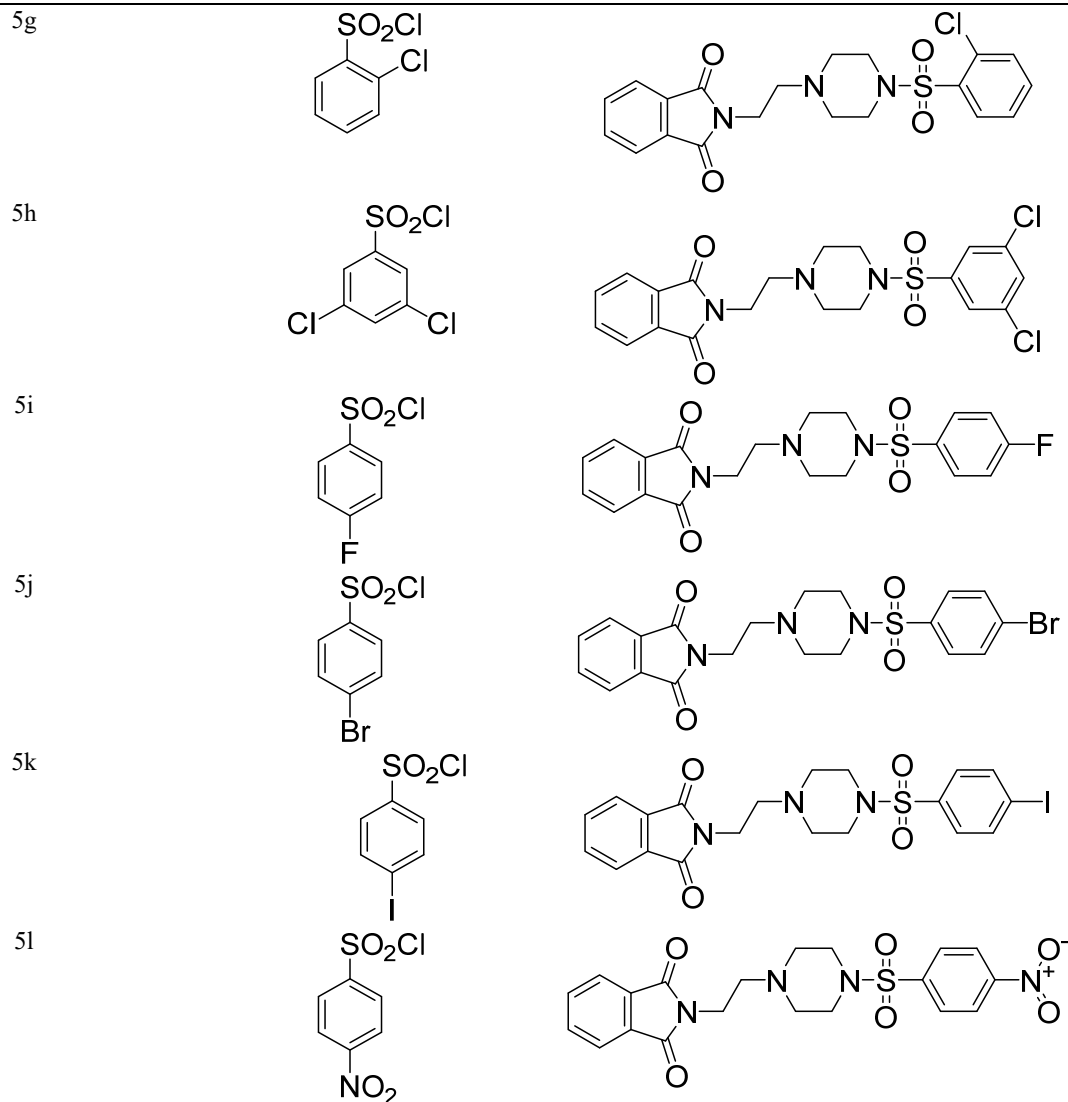


Fig. 6. Synthesis of piperazine sulfonyl derivatives

Table 5. Structure of synthesized compounds

Compound	R	Structure
5a		
5b		
5c		
5d		
5e		
5f		



4.1.2.1. 2-(2-(4-(phenylsulfonyl) piperazin-1-yl) ethyl) isoindoline-1, 3-dione (5a)

Petroleum ether/ethyl acetate (2:3) v/v solvent system has used in column chromatography. 85% yield. ¹H NMR: (400 MHz, CDCl₃) 7.88 (d, 2H, Ar-H, J=6.4Hz) 7.84 (t, 2H, Ar-H, J=7.2Hz) 7.83 (d, 2H, Ar-H, J=8.2Hz) 7.64 (t, 2H, Ar-H, J=8.4Hz) 7.63 (t, 1H, Ar-H, J=1.81Hz) 3.59 (t, 2H, C-H, J=) 3.06 (t, 4H, pip-H, J=7.1Hz) 2.60 (t, 2H, C-H, J=7.5Hz) 2.34 (t, 4H, Pip-H, J=7.2Hz). ¹³C NMR: (400Hz, CDCl₃) 167.9 (C=O), 137.0 (Ar-C), 132.2 (Ar-c), 132.0 (Ar-C), 131.9 (Ar-C), 129.0 (Ar-C), 127.3 (Ar-C), 123.7 (Ar-C), 53.7 (Pip-C), 49.8 (CH₂), 48.8 (Pip-C), 38.4 (CH₂). LCMS m/z Calculated for C₂₀H₂₁N₃O₄S: (M-H) 399.46. Found 399.49, IR Vmax (cm⁻¹) 3360 (N-H), 1720 (C=O), 1670 (C=C), 1320 (C-N), 1280 Elemental Analysis: Calculated: C, 60.14; H, 5.30; N, 10.52; O, 16.02; S, 8.03; Experimental: C, 60.15; H, 5.31; N, 10.50; O,16.01; S, 8.04

4.1.2.2. 2-(2-(4-(tosylpiperazin-1-yl) ethyl) isoindoline-1, 3-dione (5b)

Petroleum ether/ethyl acetate (2:3) v/v solvent system has used in column chromatography. 85% yield. ¹H NMR: (400 MHz, CDCl₃) 7.84 (t, 2H, Ar-H, J=7.2Hz) 7.83 (d, 2H, Ar-H, J=8.2Hz) 7.65 (d, 2H, Ar-H) 7.45 (d, 2H, Ar-H, J=7.1Hz) 3.59 (t, 2H, C-H, J=7.5Hz) 3.06 (t, 4H, Pip-H, J=7.2Hz) 2.60 (t, 2H, C-H, J=) 2.43 (d, 3H, C-H, J=) 2.34 (t, 4H, Pip-H, J=). ¹³C NMR: (400Hz, CDCl₃) 167.9 (C=O), 143.3 (Ar-C), 137.6 (Ar-C), 132.2 (Ar-C), 132.0 (Ar-C), 129.3 (Ar-C), 128.3 (Ar-C), 53.7 (Pip-C), 49.8 (CH₂), 48.8 (Pip-C), 38.4 (CH₂), 21.3 (CH₃). LCMS m/z Calculated for C₂₁H₂₃N₃O₄S: (M-H) 413.14. Found 413.49, IR Vmax (cm⁻¹) 3360 (N-H), 1720 (C=O), 1670 (C=C), 1320 (C-N). Elemental Analysis: Calculated: C, 60.14; H, 5.30; N, 10.52; O, 16.02; S, 8.03; Experimental: C, 60.10; H, 5.29; N, 10.48; O,16.02; S, 8.03

4.1.2.3. 2-(2-(4-((4-methoxyphenyl) sulfonyl) piperazin-1-yl) ethyl) isoindoline-1, 3-dione (5c)

Petroleum ether/ethyl acetate (2:3) v/v solvent system has used in column chromatography. 85% yield. ¹H NMR: (400 MHz, CDCl₃) 7.84 (t, 2H, Ar-H, J=7.2Hz) 7.83 (d, 2H, Ar-H, J=8.2Hz) 7.70 (d, 2H, Ar-H) 7.06 (d, 2H, Ar-H, J=7.1Hz) 3.81 (s, 3H, C-H, J=7.5Hz) 3.59 (t, 2H, C-H, J=7.2Hz) 3.06 (t, 4H, Pip-OH) 2.60 (t, 2H, C-H) 2.34 (t, 4H, Pip-H). ¹³C NMR: (400Hz, CDCl₃) 167.9 (C=O), 163.8 (Ar-C), 132.2 (Ar-C), 132.0 (Ar-C), 126.9 (Ar-C), 123.7 (Ar-C), 114.6 (Ar-C), 55.8 (CH₃), 53.7 (Pip-C), 49.8 (CH₂), 48.8 (Pip-C), 38.4 (CH₂). LCMS m/z Calculated for C₂₁H₂₃N₃O₅S: (M-H) 423.14. Found 423.49, IR Vmax (cm⁻¹) 3360 (N-H), 1720 (C=O), 1670 (C=C), 1320 (C-N). Elemental Analysis: Calculated: C, 60.14; H, 5.30; N, 10.52; O, 16.02; S, 8.03; Experimental: C, 60.16; H, 5.30; N, 10.51; O, 16.05; S, 8.02

4.1.2.4. 2-(2-(4-((4-hydroxyphenyl) sulfonyl) piperazin-1-yl) ethyl) isoindoline-1, 3-dione (5d)

Petroleum ether/ethyl acetate (2:3) v/v solvent system has used in column chromatography. 85% yield. ¹H NMR: (400 MHz, CDCl₃) 7.84 (t, 2H, Ar-H, J=7.2Hz) 7.83 (d, 2H, Ar-H, J=8.2Hz) 7.53 (d, 2H, Ar-H) 7.06 (d, 2H, Ar-H, J=7.1Hz) 3.59 (t, 2H, C-H, J=7.5Hz) 3.06 (t, 4H, Pip-H) 2.60 (t, 2H, C-H) 2.34 (t, 4H, Pip-H) 9.46 (s, 1H, OH). ¹³C NMR: (400Hz, CDCl₃) 167.9 (C=O), 161.7 (Ar-C), 132.3 (Ar-C), 132.2 (Ar-C), 132.0 (Ar-C), 130.0 (Ar-C), 126.5 (Ar-C), 123.7 (Ar-C), 53.7 (Pip-C), 49.8 (CH₂), 48.8 (Pip-C), 38.4 (CH₂). LCMS m/z Calculated for C₂₀H₂₁N₃O₅S: (M-H) 415.12 Found 415.46, IR Vmax (cm⁻¹) 3360 (N-H), 1720 (C=O), 1670 (C=C), 1320 (C-N). Elemental Analysis: Calculated: C, 60.14; H, 5.30; N, 10.52; O, 16.02; S, 8.03; Experimental: C, 60.14; H, 5.31; N, 10.48; O, 16.05; S, 8.01

4.1.2.5. 2-(2-(4-((4-chlorophenyl) sulfonyl) piperazin-1-yl) ethyl) isoindoline-1,3-dione (5e)

Petroleum ether/ethyl acetate (2:3) v/v solvent system has used in column chromatography. 85% yield. ¹H NMR: (400 MHz, CDCl₃) 7.84 (t, 2H, Ar-H, J=7.2Hz) 7.83 (d, 2H, Ar-H, J=8.2Hz) 7.74 (d, 2H, Ar-H) 7.61 (d, 2H, Ar-H, J=7.1Hz) 3.59 (t, 2H, C-H, J=7.5Hz) 3.06 (t, 4H, Pip-H) 2.60 (t, 2H, C-H) 2.34 (t, 4H, Pip-H). ¹³C NMR: (400Hz, CDCl₃) 167.9 (C=O), 137.8 (Ar-C), 137.5 (Ar-C), 132.2 (Ar-C), 132.0 (Ar-C), 129.1 (Ar-C), 128.7 (Ar-C), 123.7 (Ar-C), 53.7 (Pip-C), 49.8 (CH₂), 48.8 (Pip-C), 38.4 (CH₂). LCMS m/z Calculated for C₂₀H₂₀ClN₃O₄S: (M-H) 433.09 Found 433.91, IR Vmax (cm⁻¹) 3360 (N-H), 1720 (C=O), 1670 (C=C), 1320 (C-N). Elemental Analysis: Calculated: C, 60.14; H, 5.30; N, 10.52; O, 16.02; S, 8.03; Experimental: C, 60.13; H, 5.31; N, 10.52; O, 16.01; S, 8.04

4.1.2.6. 2-(2-(4-((3-chlorophenyl) sulfonyl) piperazin-1-yl) ethyl) isoindoline-1, 3-dione (5f)

Petroleum ether/ethyl acetate (2:3) v/v solvent system has used in column chromatography. 85% yield. ¹H NMR: (400 MHz, CDCl₃) 8.23 (s, 1H, Ar-H) 7.84 (t, 2H, Ar-H, J=7.2Hz) 7.83 (d, 2H, Ar-H, J=8.2Hz) 7.73 (d, 1H, Ar-H) 7.71 (d, 1H, Ar-H, J=7.1Hz) 7.54 (t, 1H, Ar-H, J=7.5Hz) 3.59 (t, 2H, C-H) 3.06 (t, 4H, Pip-H) 2.60 (t, 2H, C-H) 2.34 (t, 4H, Pip-H). ¹³C NMR: (400Hz, CDCl₃) 167.9 (C=O), 141.1 (Ar-C), 134.6 (Ar-C), 132.2 (Ar-C), 132.0 (Ar-C), 130.4 (Ar-C), 126.6 (Ar-C), 125.4 (Ar-C), 123.7 (Ar-C), 53.7 (Pip-C), 49.8 (CH₂), 48.8 (Pip-C), 38.4 (CH₂). LCMS m/z Calculated for C₂₀H₂₀ClN₃O₄S: (M-H) 433.09 Found 433.91, IR Vmax (cm⁻¹) 3360 (N-H), 1720 (C=O), 1670 (C=C), 1320 (C-N). Elemental Analysis: Calculated: C, 60.14; H, 5.30; N, 10.52; O, 16.02; S, 8.03; Experimental: C, 60.15; H, 5.31; N, 10.50; O, 16.01; S, 8.04

4.1.2.7. 2-(2-(4-((2-chlorophenyl) sulfonyl) piperazin-1-yl) ethyl) isoindoline-1,3-dione (5g)

Petroleum ether/ethyl acetate (2:3) v/v solvent system has used in column chromatography. 85% yield. ¹H NMR: (400 MHz, CDCl₃) 7.84 (t, 2H, Ar-H, J=7.2Hz) 7.83 (d, 2H, Ar-H, J=8.2Hz) 7.74 (d, 1H, Ar-H) 7.67 (d, 1H, Ar-H, J=7.1Hz) 7.63 (t, 1H, Ar-H, J=7.5Hz) 7.46 (t, 1H, Ar-H) 3.59 (t, 2H, C-H) 3.06 (t, 4H, Pip-H) 2.60 (t, 2H, C-H) 2.34 (t, 4H, Pip-H). ¹³C NMR: (400Hz, CDCl₃) 167.9 (C=O), 139.7 (Ar-C), 133.3 (Ar-C), 132.2 (Ar-C), 132.0 (Ar-C), 131.5 (Ar-C), 130.2 (Ar-C), 128.7 (Ar-C), 127.1 (Ar-C), 123.7 (Ar-C), 53.7 (Pip-C), 49.8 (CH₂), 48.8 (Pip-C), 38.4 (CH₂). LCMS m/z Calculated for C₂₀H₂₀ClN₃O₄S: (M-H) 433.09 Found 433.91, IR Vmax (cm⁻¹) 3360 (N-H), 1720 (C=O), 1670 (C=C), 1320 (C-N). Elemental Analysis: Calculated: C, 60.14; H, 5.30; N, 10.52; O, 16.02; S, 8.03; Experimental: C, 60.16; H, 5.33; N, 10.47; O, 16.02; S, 8.05

4.1.2.8. 2-(2-(4-((3,5-dichlorophenyl) sulfonyl) piperazin-1-yl) ethyl) isoindoline-1,3dione (5h)

Petroleum ether/ethyl acetate (2:3) v/v solvent system has used in column chromatography. 85% yield. ¹H NMR: (400 MHz, CDCl₃) 8.11 (s, 2H, Ar-H), 7.96 (s, 1H, Ar-H) 7.84 (t, 2H, Ar-H, J=7.2Hz) 7.83 (d, 2H, Ar-H, J=8.2Hz) 3.59 (t, 2H, C-H) 3.06 (t, 4H, Pip-H) 2.60 (t, 2H, C-H) 2.34 (t, 4H, Pip-H). ¹³C NMR: (400Hz, CDCl₃): (400Hz, CDCl₃) 167.9 (C=O), 142.5 (Ar-C), 136.0 (Ar-C), 132.4 (Ar-C), 132.2 (Ar-C), 132.0 (Ar-C), 127.7 (Ar-C), 123.7 (Ar-C), 53.7 (Pip-C), 49.8 (CH₂), 48.8 (Pip-C), 38.4 (CH₂). LCMS m/z Calculated for C₂₀H₁₉Cl₂N₃O₄S: (M-H) 467.05 Found 468.35, IR Vmax (cm⁻¹) 3360 (N-H), 1720 (C=O), 1670 (C=C), 1320 (C-N). Elemental Analysis: Calculated: C, 60.14; H, 5.30; N, 10.52; O, 16.02; S, 8.03; Experimental: C, 60.13; H, 5.32; N, 10.54; O, 16.05; S, 8.06

4.1.2.9. 2-(2-(4-((4-fluorophenyl) sulfonyl) piperazin-1-yl) ethyl) isoindoline-1,3-dione (5i)

Petroleum ether/ethyl acetate (2:3) v/v solvent system has used in column chromatography. 85% yield. ¹H NMR: (400 MHz, CDCl₃) 7.98 (d, 2H, Ar-H) 7.84 (t, 2H, Ar-H, J=7.2Hz) 7.83 (d, 2H, Ar-H, J=8.2Hz) 7.40(d, 2H, Ar-H), 3.59(t, 2H, C-H) 3.06 (t, 4H, Pip-H) 2.60 (t, 2H, C-H) 2.34 (t, 4H, Pip-H). ¹³C NMR: (400Hz, CDCl₃): (400Hz, CDCl₃) 167.9 (C=O), 166.1 (Ar-C), 135.3 (Ar-C), 132.2 (Ar-C), 132.0 (Ar-C), 130.7, 123.7 (Ar-C), 115.8 (Ar-C), 53.7 (Pip-C), 49.8 (CH₂), 48.8 (Pip-C), 38.4 (CH₂). LCMS m/z Calculated for C₂₀H₂₀FN₃O₄S: (M-H) 417.12 Found 417.46, IR Vmax (cm⁻¹) 3360 (N-H), 1720 (C=O), 1670 (C=C), 1320 (C-N). Elemental Analysis: Calculated: C, 60.14; H, 5.30; N, 10.52; O, 16.02; S, 8.03; Experimental: C, 60.15; H, 5.31; N, 10.51; O, 16.01; S, 8.03.

4.1.2.10. 2-(2-(4-((4-bromophenyl) sulfonyl) piperazin-1-yl) ethyl) isoindoline-1,3-dione (5j)

Petroleum ether/ethyl acetate (2:3) v/v solvent system has used in column chromatography. 85% yield. ¹H NMR: (400 MHz, CDCl₃) 7.89 (d, 4H, Ar-H, J=8.2Hz) 7.84(t, 2H, Ar-H), 7.83(d, 2H, Ar-H), 6.50 (d, 2H, Ar-H) 3.59 (t, 2H, C-H) 3.06 (t, 4H, Pip-H) 2.60 (t, 2H, C-H) 2.34 (t, 4H, Pip-H). ¹³C NMR: (400Hz, CDCl₃) 167.9 (C=O), 138.7 (Ar-C), 132.2 (Ar-C), 132.0 (Ar-C), 131.9 (Ar-C), 126.3 (Ar-C), 123.7 (Ar-C), 53.7 (Pip-C), 49.8 (CH₂), 48.8 (Pip-C), 38.4 (CH₂). LCMS m/z Calculated for C₂₀H₂₀BrN₃O₄S: (M-H) 477.04 Found 478.36, IR Vmax (cm⁻¹) 3360 (N-H), 1720 (C=O), 1670 (C=C), 1320 (C-N). Elemental Analysis: Calculated: C, 60.14; H, 5.30; N, 10.52; O, 16.02; S, 8.03; Experimental: C, 60.16; H, 5.33; N, 10.51; O, 16.02; S, 8.05

4.1.2.11. 2-(2-(4-((4-iodophenyl) sulfonyl) piperazin-1-yl) ethyl) isoindoline-1,3-dione (5k)

Petroleum ether/ethyl acetate (2:3) v/v solvent system has used in column chromatography. 85% yield. ¹H NMR: (400 MHz, CDCl₃) 8.02 (d, 2H, Ar-H), 7.84 (t, 2H, Ar-H), 7.83 (d, 2H, Ar-H), 7.57 (d, 2H, Ar-H), 3.59 (t, 2H, C-H) 3.06 (t, 4H, Pip-H) 2.60 (t, 2H, C-H) 2.34 (t, 4H, Pip-H). ¹³C NMR: (400Hz, CDCl₃): 167.9 (C=O), 138.6 (Ar-C), 137.9 (Ar-C), 132.2 (Ar-C), 132.0 (Ar-C), 128.9 (Ar-C), 123.7 (Ar-C), 97.5 (Ar-C), 53.7 (Pip-C), 49.8 (CH₂), 48.8 (Pip-C), 38.4 (CH₂). LCMS m/z Calculated for C₂₀H₂₀IN₃O₄S: (M-H) 525.02 Found 525.36, IR Vmax (cm⁻¹) 3360 (N-H), 1720 (C=O), 1670 (C=C), 1320 (C-N). Elemental Analysis: Calculated: C, 60.14; H, 5.30; N, 10.52; O, 16.02; S, 8.03; Experimental: C, 60.12; H, 5.30; N, 10.51; O, 16.03; S, 8.05.

4.1.2.12. 2-(2-(4-((4-nitrophenyl) sulfonyl) piperazin-1-yl) ethyl) isoindoline-1,3-dione (5l)

Petroleum ether/ethyl acetate (2:3) v/v solvent system has used in column chromatography. 85% yield. ¹H NMR: (400 MHz, CDCl₃) 8.38 (d, 2H, Ar-H), 8.05 (d, 2H, Ar-H), 7.84 (t, 2H, Ar-H), 7.83 (d, 2H, Ar-H), 3.59 (t, 2H, C-H) 3.06 (t, 4H, Pip-H) 2.60 (t, 2H, C-H) 2.34 (t, 4H, Pip-H). ¹³C NMR: (400Hz, CDCl₃) 167.9 (C=O), 151.1 (Ar-C), 145.8 (Ar-C), 132.2 (Ar-C), 132.0 (Ar-C), 128.2 (Ar-C), 124.2 (Ar-C), 123.7 (Ar-C), 53.7 (Pip-C), 49.8 (CH₂), 48.8 (Pip-C), 38.4 (CH₂). LCMS m/z Calculated for C₂₀H₂₀N₄O₆S: (M-H) 444.11 Found 444.46, IR Vmax (cm⁻¹) 3360 (N-H), 1720 (C=O), 1670 (C=C), 1320 (C-N). Elemental Analysis: Calculated: C, 60.14; H, 5.30; N, 10.52; O, 16.02; S, 8.03; Experimental: C, 60.14; H, 5.32; N, 10.51; O, 16.02; S, 8.05.

4.2. Absorption, Distribution, Metabolism and Excretion analysis and Blood-Brain Barrier permeability

The drug's effectiveness is determined not only by its great potential, but also by its proper absorption, distribution, metabolism, and excretion. Due to a wide range of experimental methodologies and high throughput, in vitro ADME screens are accessible. In silico, ADME analysis can predict many important characteristics, and it is beneficial for analysing a molecule's desirable characteristics. Because it reduces the number of safety issues, computational ADME should be employed as early as possible in the drug development process, in conjunction with in vivo and in vitro forecasts. According to Lipinski's rule, a drug candidate's molecular characteristics must be evaluated in order to determine critical pharmacokinetic factors such as ADME. Mol Inspiration, an online property calculation toolset accessible at (DOI: <http://www.molinspiration.com>), was used to forecast ADME properties.³³ The BBB permeability was evaluated by using the CBLigand-BBB prediction server available at ([DOI: http://www.cbligand.org](http://www.cbligand.org)).

4.3. Prediction of Activity Spectra for Substances test

The PASS (Prediction of Activity Spectra for Substances, ([DOI: http://www.pharmaexpert.ru/PASSonline/predict.php](http://www.pharmaexpert.ru/PASSonline/predict.php))) technique was used for statistical screening of possible biological effects, such as antihistaminic³⁴ and related behaviors, such as antiallergic, anti-asthmatic³⁵, histamine release inhibition, rhinitis treatment, Immunomodulation, bronchodilation, and anti-IgE activities, anti-IL activity, PDE inhibition, anti-5HT₃ activity, and so on. This software application created a mechanism for identifying an organic drug-like candidate's overall biological potential. PASS uses the structure of organic chemicals to represent a wide variety of biological activities in real time. Prior to chemical synthesis and biological investigation, PASS may be used to assess the biological activity profiles of virtual molecules. It forecasts the desired pharmacological impact, as well as molecular mechanisms of action and the frequency of undesirable side effects including

mutagenicity, teratogenicity, and carcinogenicity, and embryo toxicity.³⁶ By dissecting chemical structures using 2D and/or 3D descriptors, then employing bioactive ligands to construct models, this technique generated quantitative structure-activity connections. This program generated quantitative structure-activity connections by deconstructing chemical compounds using 2D and/or 3D descriptors and then employing bioactive ligands to construct models. The activity was measured using PA (probable activity) and Pi (potential activity) (probable inactivity). Only compounds having a Pa larger than Pi were examined for a specific application.

4.4. Antibacterial activity against MRSA

Susceptibility testing was carried out using the Kirby Bauer disc diffusion technique in accordance with Clinical Laboratory Standard Institute (CLSI) criteria from 2016. In sterile normal saline, the inoculums were prepared and suspended. By comparing the density of the suspension to an opacity standard on McFarland 0.5 barium sulfate solution, the density of the suspension was determined. The research organism was uniformly seeded over the Mueller–Hinton agar (Oxoid) surface and subjected to an antibiotic concentration gradient before being incubated for 16–18 hours at 37°C. The diameters of the region of inhibition around the discs were determined with a ruler to the nearest millimeter and graded as sensitive, intermediate, or resistant using the CLSI, standardized table. Ciprofloxacin (5 g), gentamicin (10 g), tetracycline (30 g), co-trimoxazole (25 g), chloramphenicol (30 g), amikacin (30 g), clindamycin (10 g), erythromycin (15 g), and vancomycin (30 g) were among the antibiotics studied.³⁷ The antimicrobials used in this research were chosen based on their availability and prescription frequency in the study field.

4.4.1. Preparation of bacterial culture and maintenance

A single pure colony was used, which was obtained from a frozen glass bead glycerol vial (previously culture coated on glass beads and stored at -18° to -22° C). The pure culture was inoculated into BHI broth and incubated for 24 hours at 37° C. The cell density was adjusted to 1×10^6 CFU/mL using UV-vis spectroscopy at 600 nm.³⁸

4.4.2. Minimum inhibitory concentration by resazurin assay

The Minimal inhibitory concentration (MIC) of produced piperazine sulphonyl derivatives was used in the Resazurin assay. In the assay 100µL of sterile BHI broth was placed in each of the 96 wells. Sulphonyl derivatives were dissolved in dimethyl sulfoxide (DMSO) and mixed with media in varied quantities. Each well received a 10 µL resazurin indicator solution (270 mg in 40 mL sterilized distilled water). Finally, 10µL of bacterial suspension (5×10^6 CFU/mL) were added, to give 5×10^5 CFU/mL and two broad-spectrum antibiotics such as Streptomycin and Bacitracin were used as Standard bactericidal agents. A combination with all additions except the test chemical was utilized as a positive control. Similarly, negative controls included all solutions without the addition of bacterial culture. The plates were covered in thin plastic film and incubated for 24h at 37°C.³⁹

4.4.3. Disc diffusion method

The disc diffusion method was used to evaluate the antibacterial activity of synthesized piperazine and sulphonyl derivatives in a dose-dependent way to susceptibility. The bacterial cultures were prepared from the overnight grown dynamic culture. The test culture of 1×10^7 CFU mL⁻¹ was inoculated on nutrient agar. To this, a sterile disc (6 mm) was loaded with various concentrations of piperazine and sulphonyl derivatives. The Positive control was streptomycin (10 g disc1), and the negative control was sterile saline water. The plates were inverted and incubated at 37°C for 24 hours to examine the zone of inhibition (ZOI).⁴⁰

4.4.4. MRSA membrane damage visualized by SEM

Scanning electron microscopy (SEM) was used to demonstrate membrane damage studies of MRSA.⁴¹ This freshly grown MRSA culture was treated for 2 h with the lowest inhibitory concentration of sulphonyl derivatives. Then the cells were pelleted by centrifugation at 27° C (10000 rpm for 5 min). MRSA culture was prepared without treatment as a control. Phosphate buffered saline (PBS) with 2.5% Glutaraldehyde was used to fix the cells. This was then pelleted and deposited on a glass slide followed by a stepwise ethanol drying treatment of 30% to 100%. This is then followed by two days of drying at room temperature. The prepared sample was used for SEM studies.

4.5. Molecular docking validation

The RCSB Protein Data Bank was used to obtain the coordinates of wild-type 3VMT and the 6FTB of *Staphylococcus aureus*. The crystal structure was refined or synthesized in a multistep approach using Maestro 9.3 software's protein preparation wizard, which includes energy minimization. The correct bond ordering was assigned using the OPLS-2005 force field, hydrogen atoms were added, and water molecules were eliminated beyond 5Å from the hetero atom, formal charges, and amide groups of Asn and Gln were optimized. The hydrogen bonds were enhanced and all amino acid flips were allocated to address geometry. The pH was fixed and tuned to 7.5 using PROPKA. The controlled reduction was used

to reduce non-hydrogen atoms to a default RMSD of 0.3. Each chemical was docked into the receptor grid of radii 30Å x 30Å x 30Å using extra-accuracy (XP) docking and scoring, and the docking computation was judged based on the Glide score.⁴²

4.6. Toxicity of 5e and sulphonyl derivatives against L6 cell lines

4.6.1 Preparation of L6 cell lines and MTT assay

Using recommended media containing 10% FBS (Fetal Bovine Serum) the monolayer cell culture was trypsinized and the cell count was adjusted to 5.0×10^5 cells/ml. A 96-well microtiter plate was filled with 100µL of diluted cell solution (50,000 cells/well). The supernatant was flicked off, the monolayer was rinsed once with media, and 100 µL of different concentrations of test drugs were combined with cell line culture after 24 hours when a partial monolayer had developed. In a 5% CO₂ environment, the plate was incubated at 37°C for 24 hours. The test solutions in the wells were removed after incubation, and 100 µL of MTT (5 mg/10 mL in PBS) was added to each well. The plates were incubated for 4 hours at 37°C in a 5% CO₂ environment. Then the supernatant was removed, 100 µL of DMSO was added, and the plate was gently agitated to dissolve the Formosan which had formed. At a wavelength of 590 nm, the absorbance was taken using a micro plate reader. The percentage growth inhibition was estimated using the concentration of test medication required to stop cell growth in a cell line by 50 % (IC₅₀).⁴³

References

- Bergdoll M.S. (1991) Staphylococcus aureus. *J. AOAC Int.*, 74(4), 706-710. (DOI:<https://doi.org/10.1093/jaoac/74.4.706>).
- Campoccia D., Montanaro L., and Arciola C.R. (2013) A review of the clinical implications of anti-infective biomaterials and infection-resistant surfaces. *Biomaterials.*, 34(33), 8018-8029. (DOI:<https://doi.org/10.1016/j.biomaterials.2013.07.048>).
- Lowy FD. (1998) Staphylococcus aureus infections. *New Eng. J. Med.*, 339(8), 520-532. (DOI: [10.1056/NEJM199808203390806](https://doi.org/10.1056/NEJM199808203390806)).
- Dantas G., Sommer M.O., Oluwasegun R.D., Church G.M. (2008) Bacteria subsisting on antibiotics. *Science.*, 320(5872), 100-103. (DOI: [10.1126/science.1155157](https://doi.org/10.1126/science.1155157)).
- Berg A.T., Shapiro E.D., Capobianco L.A. (1991) Group Day care and the risk of serious infectious illnesses. *Am. J. Epidemiol.*, 133(2), 154-163. (DOI: <https://doi.org/10.1093/oxfordjournals.aje.a115854>).
- De Oliveira D.M., Forde B.M., Kidd T.J., Harris P.N., Schembri M.A., Beatson S.A., Walker M.J. (2020) Antimicrobial resistance in ESKAPE pathogens. *Clin. Microbiol. Rev.*, 33(3), 00181-19. (DOI: <https://doi.org/10.1128/CMR.00181-19>).
- Garrod L.P. (1957) The erythromycin group of antibiotics. *BMJ.*, 2(5036):57. (DOI: <https://doi.org/10.1136/bmj.2.5036.57>).
- Kasten, M. J. (1999, August). Clindamycin, metronidazole, and chloramphenicol. In *Mayo Clin. Proc.*, 74(8), 825-83. (DOI: <https://doi.org/10.4065/74.8.825>).
- Turel I., Bukovec P., Quirós (1997) Crystal structure of ciprofloxacin hexahydrate and its characterization. *Int. J. Pharm.*, 152(1), 59-65. (DOI: [https://doi.org/10.1016/S0378-5173\(97\)04913-2](https://doi.org/10.1016/S0378-5173(97)04913-2)).
- Mendez B., Tachibana C., Levy S.B. (1980) Heterogeneity of tetracycline resistance determinants. *Plasmid.* 3(2), 99-108. (DOI:[https://doi.org/10.1016/0147-619X\(80\)90101-8](https://doi.org/10.1016/0147-619X(80)90101-8)).
- Mediavilla J.R., Chen L., Mathema B., Kreiswirth B.N. (2012) Global epidemiology of community-associated methicillin resistant Staphylococcus aureus (CA-MRSA). *Current opinion in microbiology*, 15(5), 588-595. (DOI: <https://doi.org/10.1016/j.mib.2012.08.003>).
- Enright M.C., Robinson D.A., Randle G., Feil E.J., Grundmann H., Spratt B.G. (2002) The evolutionary history of methicillin-resistant Staphylococcus aureus (MRSA). *Proc. Natl. Acad. Sci.*, 99(11), 7687-7692. (DOI: <https://doi.org/10.1073/pnas.122108599>).
- Davis K.A., Stewart J.J., Crouch H.K., Florez C.E., Hospenthal D.R. (2004) Methicillin-resistant Staphylococcus aureus (MRSA) nares colonization at hospital admission and its effect on subsequent MRSA infection. *Arch. Clin. Infect. Dis.* 39(6), 776-782. (DOI: <https://doi.org/10.1086/422997>).
- Bal A.M., David M.Z., Garau J., Gottlieb T., Mazzei T., Scaglione F., Gould IM. (2019) Future trends in the treatment of methicillin-resistant Staphylococcus aureus (MRSA) infection: an in-depth review of newer antibiotics active against an enduring pathogen. *J. Glob. Antimicrob. Resist.* 10, 295-303. (DOI: <https://doi.org/10.1016/j.jgar.2017.05.019>).
- Foroumadi A., Emami S., Mansouri S., Javidnia A., Saeid-Adeli N., Shirazi F.H., Shafiee A. (2007) Synthesis and antibacterial activity of levofloxacin derivatives with certain bulky residues on piperazine ring. *Eur. J. Med. Chem.* 42(7), 985-992. (DOI: <https://doi.org/10.1016/j.ejmech.2006.12.034>).
- Prasad H. N., Ananda A. P., Lohith T. N., Prabhuprasad P., Jayanth H. S., Krishnamurthy N. B. & Mallu P. (2022). Design, synthesis, molecular docking and DFT computational insight on the structure of Piperazine sulfynol

- derivatives as a new antibacterial contender against superbugs MRSA. *J. Mol. Struct.*, 1247, 131333. (DOI: <https://doi.org/10.1016/j.molstruc.2021.131333>).
17. Rathi A.K., Syed R., Shin H.S., Patel R.V. (2016) Piperazine derivatives for therapeutic use: a patent review (2010). *Expert Opin. Ther. Pat.* 26(7), 777-797. (DOI: <https://doi.org/10.1080/13543776.2016.1189902>).
 18. Brito A.F., Moreira L.K., Menegatti R., Costa E.A. (2019) Piperazine derivatives with central pharmacological activity used as therapeutic tools. *Fundam Clin Pharmacol.*, 33(1), 13-24. (DOI: <https://doi.org/10.1111/fcp.12408>).
 19. Kushwaha N., Kaushik D. (2016) Recent advances and future prospects of phthalimide derivatives. *J. Appl. Pharm. Sci.* 6(03), 159-171. (DOI: [10.7324/JAPS.2016.60330](https://doi.org/10.7324/JAPS.2016.60330)).
 20. Othman I.M., Gad-Elkareem M.A., El-Naggar M., Nossier E.S., Amr A.E.G.E. (2019) Novel phthalimide based analogues: Design, synthesis, biological evaluation, and molecular docking studies. *J Enzyme Inhib Med Chem.*, 34(1), 1259-1270. (DOI: <https://doi.org/10.1080/14756366.2019.1637861>).
 21. Sangwan S, Yadav N, Kumar R, Chauhan S, Dhanda V, Walia P, Duhan A. (2022) A score years' update in the synthesis and biological evaluation of medicinally important 2-pyridones. *Eur. J. Med. Chem.*, 114-199. (DOI: <https://doi.org/10.1016/j.ejmech.2022.114199>).
 22. Prasad, H. N., Ananda, A. P., Sumathi, S., Swathi, K., Rakesh, K. J., Jayanth, H. S., & Mallu, P. (2022). Piperazine selenium nanoparticle (Pipe@ SeNP's): A futuristic anticancer contender against MDA-MB-231 cancer cell line. *J. Molec. Struct.*, 1268, 133683. (DOI: doi.org/10.1016/j.molstruc.2022.133683).
 23. Efimov A.M., Pogareva V.G. (2006) IR absorption spectra of vitreous silica and silicate glasses: The nature of bands in the 1300 to 5000 cm⁻¹ regions. *Chem. Geol.*, 229(1-3), 198-217. (DOI: <https://doi.org/10.1016/j.chemgeo.2006.01.022>).
 24. Santos F.D., Abreu P., Castro H.C., Paixão I.C., Cirne-Santos C.C., Giongo V., Barbosa J.E., Simonetti B.R., Garrido V., Bou-Habib D.C., Silva D.D. (2009) Synthesis, antiviral activity and molecular modeling of oxoquinoline derivatives. *Bioorg. Med. Chem.*, 17(15), 5476-81. (DOI: <https://doi.org/10.1016/j.bmc.2009.06.037>).
 25. Jia C.Y., Li J.Y., Hao G.F., Yang G.F. (2020) A drug-likeness toolbox facilitates ADMET study in drug discovery. *Drug Discov. Today.* 25(1), 248-258. (DOI: <https://doi.org/10.1016/j.drudis.2019.10.014>).
 26. Xu X., Du C., Ma F., Shen Y., Zhou J. (2020) Forensic soil analysis using laser-induced breakdown spectroscopy (LIBS) and Fourier transform infrared total attenuated reflectance spectroscopy (FTIR-ATR): principles and case studies. *Forensic Sci. Int.*, 310, 110222. (DOI: <https://doi.org/10.1016/j.forsciint.2020.110222>).
 27. Dash S., Borah S.S., & Kalamdhad A.S. (2020) Application of positive matrix factorization receptor model and elemental analysis for the assessment of sediment contamination and their source apportionment of DeeporBeel. *Ecol. Indic.*, 114, 106291. (DOI: <https://doi.org/10.1016/j.ecolind.2020.106291>).
 28. Girase P.S., Dhawan S., Kumar V., Shinde S.R., Palkar M.B., Karpoornath R. (2021) An appraisal of anti-mycobacterial activity with structure-activity relationship of piperazine and its analogues: A review. *Eur. J. Med. Chem.* 210, 112967. (DOI: <https://doi.org/10.1016/j.ejmech.2020.112967>).
 29. Prasad, H. S. N., Gaonkar, N. P., Ananda, A. P., Mukarambi, A., Kumar, G. C., Lohith, T. N., & Beeregowda, N. (2022). Antibacterial Property of Schiff-based Piperazine against MRSA: Design, Synthesis, Molecular Docking, and DFT Computational Studies. *Lett. Appl. NanoBioScience*, 2, 54. (<https://doi.org/10.33263/LIANBS122.054>).
 30. Xu Z. (2020) 1, 2, 3-Triazole-containing hybrids with potential antibacterial activity against methicillin-resistant Staphylococcus aureus (MRSA). *Eur. J. Med. Chem.*, 112686. (DOI: <https://doi.org/10.1016/j.ejmech.2020.112686>).
 31. Prasad H.N., Karthik C.S., Manukumar H.M., Mallesha L., Mallu P. (2019) New approach to address antibiotic resistance: Miss loading of functional membrane microdomains (FMM) of methicillin-resistant Staphylococcus aureus (MRSA). *Microb. Pathog.*, 127, 106-115. (DOI: <https://doi.org/10.1016/j.micpath.2018.11.038>).
 32. Santoro F., Zhao W., Joubert L.M., Duan L., Schnitker J., van de Burgt Y., Cui B. (2017) Revealing the cell-material interface with nanometer resolution by focused ion beam/scanning electron microscopy. *ACS nano.*, 11(8), 8320-8328. (DOI: <https://doi.org/10.1021/acs.nano.7b03494>).
 33. Darvas F, Keseru G, Papp A, Dorman G, Urge L, Krajcsi P. (2002) In silico and ex silico ADME approaches for drug discovery. *Curr. Top. Med. Chem.*, 2(12):1287-1304. (DOI: <https://doi.org/10.2174/1568026023392841>).
 34. Gurjar V.K., Pal D. (2020) Design, in silico studies, and synthesis of new 1, 8-naphthyridine-3-carboxylic acid analogues and evaluation of their H1R antagonism effects. *RSC Advances.*, 10(23), 13907-21. (DOI: <https://doi.org/10.1039/D0RA00746C>).
 35. Merlob P., Weber-Schöndorfer C. (2015) Antiallergics, Antiasthmatics and antitussives. *Drugs During Pregnancy and Lactation.*, 671-676. (DOI: <https://doi.org/10.1016/B978-0-12-408078-2.00027-5>).
 36. Parasuraman S. (2011) Prediction of activity spectra for substances. *J Pharmacol Pharmacother*, 2(1), 52. (DOI: <https://doi.org/10.4103/2F0976-500X.77119>).

37. Joshi P.R., Acharya M, Aryal R, Thapa K, Kakshapati T, Seng R, Singh A, Sitthisak S. (2017) Emergence of staphylococcal cassette chromosome mec type I with high-level mupirocin resistance among methicillin-resistant *Staphylococcus aureus*. *Asian Pac. J. Trop. Biomed.*, 7(3), 193-7. (DOI: <https://doi.org/10.1016/j.apitb.2016.12.002>).
38. Berninger T., González López Ó., Bejarano., Preininger C., Sessitsch A. (2018) Maintenance and assessment of cell viability in formulation of non-sporulating bacterial inoculants. *Microbial biotechnology.*, 11(2), 277-301. (DOI: <https://doi.org/10.1111/1751-7915.12880>).
39. Manuel A., Abdulrahman N. (2017) Determination of Minimum Inhibitory Concentration of Liposomes: A Novel Method. *Int. J. Curr. Microbiol. App. Sci.*, 6(8), 1140-1147. (DOI: <http://dx.doi.org/10.20546/ijcmas.2017.602.141>).
40. Jonasson E., Matuschek E., Kahlmeter G. (2020) The EUCAST rapid disc diffusion method for antimicrobial susceptibility testing directly from positive blood culture bottles. *J. Antimicrob. Chemother.*, 75(4), 968-978. (DOI: <https://doi.org/10.1093/jac/dkz548>).
41. Ansari, M. A., & Alzohairy, M. A. (2018). One-pot facile green synthesis of silver nanoparticles using seed extract of *Phoenix dactylifera* and their bactericidal potential against MRSA. *Evid Based Complement Alternat Med.*, 2018. (DOI: <https://doi.org/10.1155/2018/1860280>).
42. Deb P.K., Al-Shar'i N.A., Venugopala K.N., Pillay M, Borah P. (2021) In vitro anti-TB properties, in silico target validation, molecular docking and dynamics studies of substituted 1, 2, 4-oxadiazole analogues against *Mycobacterium tuberculosis*. *J Enzyme Inhib Med Chem.*, 36(1), 869-884. (DOI: <https://doi.org/10.1080/14756366.2021.1900162>).
43. Miranda C.L., Stevens J.F., Helmrich A., Henderson M.C., Rodriguez R.J., Yang Y.H., Deinzer M.L., Barnes D.W., Buhler D.R. (1999) Antiproliferative and cytotoxic effects of prenylated flavonoids from hops (*Humulus lupulus*) in human cancer cell lines. *Food Chem. Toxicol.*, 37(4), 271-85. (DOI: [https://doi.org/10.1016/S0278-6915\(99\)00019-8](https://doi.org/10.1016/S0278-6915(99)00019-8)).



© 2023 by the authors; licensee Growing Science, Canada. This is an open access article distributed under the terms and conditions of the Creative Commons Attribution (CC-BY) license (<http://creativecommons.org/licenses/by/4.0/>).